GRP Receptor-Targeted PET of a Rat Pancreas Carcinoma Xenograft in Nude Mice with a ^{68}Ga-Labeled Bombesin(6–14) Analog

Jochen Schuhmacher, PhD[1]; Hanwen Zhang, MS[2]; Josef Doll, PhD[1]; Helmut R. Mäcke, PhD[2]; Ronald Matys, BSc[1]; Harald Hauser, BSc[1]; Marcus Henze, MD[3]; Uwe Haberkorn, MD[3]; and Michael Eisenhut, PhD[1]

[1]Department of Diagnostic and Therapeutic Radiology, German Cancer Research Center, Heidelberg, Germany; [2]Institute of Nuclear Medicine, University Hospital Basel, Basel, Switzerland; and [3]Department of Nuclear Medicine, University of Heidelberg, Heidelberg, Germany

Bombesin (BN), a 14-amino-acid peptide, shows high affinity for the human gastrin-releasing peptide receptor (GRP-r), which is overexpressed on several types of cancer, including prostate, breast, gastrointestinal, and small cell lung cancer. Thus, radiolabeled BN or BN analogs may prove to be specific tracers for diagnostic and therapeutic targeting of GRP-r–positive tumors in nuclear medicine. This study evaluated a novel BN analog labeled with the positron emitter ^{68}Ga for receptor imaging with PET. **Methods:** DOTA-PEG$_2$-[D-Tyr^6,β-Ala^{11},Thi^{13},Nle^{14}] BN(6–14) amide (BZH3) (DOTA is 1,4,7,10-tetraazacyclododecane-*N,N′,N″,N‴*-tetraacetic acid; PEG is ethyleneglycol (2-aminoethyl)carboxymethyl ether) was synthetized using the Fmoc strategy and radiolabeled with either ^{67}Ga or ^{177}Lu for in vitro and biodistribution experiments. ^{68}Ga for PET was obtained from a ^{68}Ge/^{68}Ga generator. In vitro binding, internalization, and efflux were determined using the pancreatic tumor cell line AR42J. Biodistribution of the peptide as a function of time and dose was studied in AR42J tumor-bearing mice. **Results:** In vitro assays demonstrated a high affinity of ^{67}Ga-BZH3 (dissociation constant = 0.46 nmol/L), a rapid internalization (70% of total cell-associated activity was endocytosed after a 15-min incubation), and an intracellular retention half-life ($t_{1/2}$) of the ^{67}Ga activity of 16.5 ± 2.4 h. Biodistribution indicated a dose-dependent uptake in the tumor and a prolonged tumor residence time ($t_{1/2} \sim$ 16 h). Clearance from GRP-r–negative tissues was fast, resulting in high tumor-to-tissue ratios as early as 1 h after injection. Replacing ^{67}Ga by ^{177}Lu, a therapeutic radionuclide, for peptide labeling resulted in a slightly reduced ($\sim$20%) tumor uptake and tumor residence time of ^{177}Lu-BZH3. In contrast, ^{177}Lu decline in the pancreas was significantly accelerated by a factor of $\sim$3 compared with that of ^{67}Ga. PET of mice with ^{68}Ga-BZH3 clearly delineated tumors in the mediastinal area. **Conclusion:** The promising in vivo data of ^{68}Ga-BZH3 indicate its potential for an improved localization of GRP-r–positive tumors and also suggest its application in patients. PET may also be favorably used for GRP-r density determination, a prerequisite for therapeutic applications.

Bombesin (BN) is an amphibian neuropeptide of 14 amino acids that shows—just as its mammalian homolog gastrin-releasing peptide (GRP)—high affinity for the human GRP receptor (GRP-r). Aside from its physiologic actions on the central nervous system (*1*) and the release of gastrointestinal hormones (*2*), BN acts as an autocrine growth stimulator in a variety of human neoplasms (*3–5*). Autoradiographic examination of malignant tissues using radioiodine-labeled BN or BN analogs demonstrated a high GRP-r expression in prostate, gastrointestinal, breast, and small cell lung cancer specimens compared with the surrounding normal tissues (*6–12*), suggesting the potential of GRP-r for a specific tumor targeting. Consequently, various radiolabeled BN analogs have been investigated and proposed for use in nuclear medicine (*13–20*). In particular, ^{90}Y, ^{188}Re, and ^{177}Lu have been used to radiolabel BN analogs for potential radiotherapy applications, whereas ^{99m}Tc and ^{111}In labeling has been used for γ-camera imaging of GRP-r–positive tumors.

PET is the most efficient imaging method in nuclear medicine because of its option of an absolute activity determination, its better contrast resolution, and its higher detection efficiency compared with conventional γ-cameras. Thus, we have focused on the labeling of BN analogs with the short-lived positron emitter ^{68}Ga (half-life [$t_{1/2}$] = 68 min; β$^+$, 88%), which is obtained from a ^{68}Ge/^{68}Ga radionuclide generator. In the present study, we evaluated a novel BN analog (BZH3) derivatized with the macrocyclic chelator 1,4,7,10-tetraazacyclododecane-*N,N′,N″,N‴*-tetraacetic acid (DOTA). This ligand forms M^{3+} metal chelates of high in vivo stability and can be labeled with $^{68/67}$Ga, ^{111}In, ^{90}Y, and ^{177}Lu and, thus, is suitable for diagnostic and therapeutic applications as well.

MATERIALS AND METHODS

Synthesis and Radiolabeling of BZH3

All chemicals were purchased from commercial sources and used without further purification. DOTA-Tris (tBu ester) was obtained from Macrocyclics. Rink amide MBHA (4-methylbenz-hydrylamine) resin and all Fmoc-protected amino acids were available from Novabiochem and Neosystem, respectively. Peptide synthesis was performed on a semiautomatic peptide synthesizer (Rink Combichem Technologies) according to general Fmoc chemistry. The peptide was assembled on a Rink amide MBHA resin. Trityl (Trt) and tBu were used as protecting groups of His and D-Tyr, respectively, and Boc was used for Trp. The spacer (Fmoc-PEG$_2$-OH [PEG is ethyleneglycol (2-aminoethyl)car-boxymethyl ether]) was coupled to the chelator DOTA-Tris (tBu ester) as described previously (21). The peptide chelator conjugate was cleaved from the resin and deprotected by incubation with trifluoroacetic acid (TFA)/thioanisole/water, 92:6:2 for 4–6 h at room temperature, and precipitated in isopropyl ether/petroleum ether (1:1). The crude peptide-chelator conjugate was purified by preparative high-performance liquid chromatography (HPLC) on a Nucleosil 100-5 C$_{18}$ column (Macherey–Nagel) at a flow rate of 15 mL/min (eluents: A = 0.1% TFA in water and B = acetonitrile; nonlinear gradient: 0 min, 70% A; 10 min, 50% A). Mass spec-tometry (MS-MALDI) was used to characterize the composition of the conjugate.

^{68}Ga for PET was obtained from a ^{68}Ge/^{68}Ga generator, which consists of a column containing a self-made phenolic ion-ex-changer loaded with ^{68}Ge and coupled in series with a small-sized anion-exchanger column (AG 1×8 Cl$^-$, mesh 200–400; Bio-Rad) to concentrate ^{68}Ga during elution (22). This generator provides ^{68}Ga with an average yield of ~60% for >1.5 y. For peptide labeling, the eluate containing ~0.5 GBq of ^{68}Ga in 0.2 mL 0.5 mol/L HCl was evaporated to dryness and redissolved in 0.2 mL 0.1 mol/L acetate buffer (pH 4.8). After addition of 5 µL 1 mmol/L aqueous solution of BZH3, the mixture was kept for 10 min at 90°C. Uncomplexed ^{68}Ga was separated by adsorption onto a C$_{18}$-coated silica gel cartridge (Sep-Pak; Waters Corp.) that was equilibrated with 0.1 mol/L acetate buffer (pH 6.2), whereas ^{68}Ga-BZH3 could be eluted with 1.5 mL ethanol. After evaporation of the organic solvent, the compound was redissolved in 0.01 mol/L phosphate-buffered saline ([PBS] pH 7.) containing 0.5 mg/mL human serum albumin. The preparations were checked for bound and free ^{68}Ga by paper chromatography using Whatman no. 1 and a mixture of methanol and 0.01 mol/L acetate buffer (pH 6.2) at a ratio of 55:45. ^{68}Ge contamination of the ^{68}Ga-BZH3 preparations was determined by γ-counting after a waiting period of ≥30 h, which ensures complete ^{68}Ga decay. ^{67}GaCl$_3$ and ^{177}LuCl$_3$ used for in vitro and biodistribution experiments were obtained in dilute HCl from Mallinckrodt and Perkin Elmer, respectively. All label-ing steps with these radionuclides were identical to that of ^{68}Ga. The radiochemical purity of ^{67}Ga-BZH3 was analyzed by re-versed-phase HPLC using a Nucleosil 120 C$_{18}$ column (Macherey–Nagel) at a flow rate of 0.75 mL/min (eluents: A = 0.1% TFA in water; B = acetonitrile; nonlinear gradient: 0 min, 80% A; 20 min, 50% A).

Cell Lines

For all in vivo and in vitro experiments, the AR42J cell line, derived from a rat exocrine pancreas tumor, was used. Cells were obtained from the European Collection of Cell Cultures and were grown in RPMI 1640 medium supplemented with 2 mmol/L glu-tamine and 10% fetal calf serum. Adherent cells were dislodged with trypsin/ethylenediaminetetraacetic acid (0.02%:0.05%, w/v) and allowed to recover for 2 h. Nonspecific binding of ^{67}Ga-BZH3 was tested with the GRP-r–negative human breast carcinoma cell line AR-1, obtained from the Department of Gynecological On-cology (University Hospital Heidelberg, Heidelberg, Germany).

Receptor Binding

The equilibrium binding constant, K_a, of ^{67}Ga-BZH3 to the GRP-rs of AR42J cells was determined using a fixed number of 4×10^5 cells in 150 µL RPMI 1640 medium and increasing amounts, 0.033–1.056 pmol (0.055–1.76 ng), of the peptide. Cells were placed in a U-shaped 96-well plate and agitated on a gyratory shaker for 1 h in an incubator (37°C, 5% CO$_2$). Cells were washed 3 times with ice-cold RPMI 1640 medium and pellets were counted in a γ-counter. A least-squares fit from a Scatchard plot (bound activity/free activity [B/F] vs. bound activity [B]) results in a straight line, the slope of which indicates $-K_a$. The intercept of B/F with B represents the maximum concentration of peptide (B$_{max}$) bound to the GRP-rs of cells at infinite peptide excess.

Internalization

Internalization of ^{67}Ga-BZH3 was studied at low and high peptide-to-receptor ratios. Twenty-seven million cells in 8.1 mL medium were incubated (37°C, 5% CO$_2$) with either 0.45 or 45 pmol (0.75 or 75 ng) of the peptide. During incubation, cells were kept in suspension by gyratory shaking. After 15, 30, 60, and 120 min of incubation, six 300-µL samples, containing 1×10^6 cells and 0.0166 or 1.66 pmol of peptide, were taken, mixed with 700 µL ice-cold RPMI 1640 medium in a conical tube, and centrifuged (3 min, 500g). Three samples were washed twice with 1 mL ice-cold RPMI 1640 medium, and cell pellets were counted in a γ-counter. Radioactivity in the cell pellets represents surface bound together with internalized peptide. The remaining 3 samples were further incubated (5 min, 22°C) with 1 mL of an acidic buffer (pH 4.3) containing 0.15 mol/L NaCl, 0.02 mol/L NaOAc, and 2 mg/mL human serum albumin to remove surface-bound peptide (23). Subsequently, cells were washed twice with the acidic buffer. Radioactivity in the cell pellet was assumed to represent internal-ized peptide

Efflux

Since an acid treatment of cells might unfavorably affect cell metabolism (23), we used an excess of unlabeled BZH3 to remove surface-bound radioactive peptide before efflux determination, which additionally blocks rebinding of internalized radioactivity released from the cells during incubation. Sixteen million cells in 4.8 mL RPMI 1640 medium were preloaded with 10 pmol of either ^{67}Ga- or ^{177}Lu-labeled BZH3 for 1 h at 37°C, 5% CO$_2$. Cells were washed 3 times and then resuspended in 4.8 mL medium; two 300-µL samples were taken as a control for total cell-associated activity (cell surface bound and internalized). Subsequently, 50 µL of 1 mmol/L unlabeled BZH3 were added to the remaining incu-bation mixture. Ten, 20, 30, 60, 90, and 120 min after the addition of unlabeled peptide, two 303-µL samples (1×10^6 cells) were taken, diluted with 700 µL ice-cold RPMI 1640 medium, and centrifuged. Pellets were washed twice with cold medium and counted for radioactivity.

Receptor Density

Since the receptor density of AR42J cells might decrease with increasing passages, accompanied by a reduction in cellular size

and tumorigenic activity, the binding capacity of cells was tested before each tumor inoculation. One million cells in 150 μL RPMI 1640 medium were incubated with 1.5 pmol of ^{67}Ga-BZH3, kept in suspension for 1 h at 37°C, 5% CO_2, washed 3 times with cold medium, and counted for radioactivity.

Biodistribution

Animal experiments were performed in accordance with the German laws for the protection of animals. Female Swiss CD1 *nu/nu* mice (8-wk old; Iffa Credo) had subcutaneous inoculation of 5×10^6 AR42J tumor cells (in 0.2 mL of RPMI 1640 medium) into the right thoracic wall near the shoulder. Eleven to 13 d later, tumors that weighed 100–600 mg were selected for the experiments. Mice received a tail vein injection of 0.2 mL 0.01 mol/L PBS containing 100 μg human serum albumin and the labeled compounds under investigation. Animals were anesthetized with ether, bled from the retroorbital plexus, and killed by cervical dislocation at the time points indicated. Organs were removed, weighed, and counted for radioactivity with a high-resolution germanium detector. For evaluation of a dose dependence of the tumor uptake, mice were injected with 5, 15, 45, or 135 pmol of ^{67}Ga-BZH3 and killed 1 h after injection. Biokinetics were studied in animals receiving a 15-pmol dose of either ^{67}Ga- or ^{177}Lu-labeled BZH3. Mice were killed 1, 2, 4, and 24 h after injection of ^{67}Ga-BZH3 and 1 and 24 h after injection of ^{177}Lu-BZH3. GRP-r–blocking studies were performed using AR42J tumor-bearing male Lewis rats (body weight, 160–200 g; Iffa Credo) as described previously (*24*). Briefly, 2 groups of rats, each comprising 4 animals, were injected with either 60 pmol (0.1 μg) ^{177}Lu-BZH3 or a mixture containing 0.1 μg ^{177}Lu- BZH3 and 50 μg of unlabeled BZH3. Rats were killed 4 h after injection. Pancreas and tumor were dissected and counted for ^{177}Lu activity.

PET

AR42J tumor-bearing mice were injected with 15 pmol (0.49 MBq) ^{68}Ga-BZH3, sacrificed 1 h after injection, and imaged with a 30-min emission scan and a 10-min transmission scan on an ECAT EXACT HR$^+$ scanner (Siemens/CTI). Images were taken in the 3-dimensional (3D) mode and reconstructed iteratively with a fully 3D algorithm from a 256×256 matrix for viewing transaxial, coronal, and sagittal slices of 0.57-mm thickness (*25*). Pixel size was 1.14 mm and transaxial resolution obtained was 2.8 mm. Subsequently, tumors were removed and counted for ^{68}Ga activity.

RESULTS

Synthesis and Radiolabeling

BZH3 (Fig. 1) was synthesized using the Fmoc strategy affording an overall yield of 30% based on the removal of the first Fmoc group; the purity analyzed by HPLC was ≥97%. MS-MALDI confirmed the calculated exact mass of 1,669.79: m/z (%): 1,670.0 (100, [M+H]$^+$); 1,692.0 (19, [M+Na]$^+$); 1,708.9 (10, [M+K]$^+$). Labeling of BZH3 with M^{3+} radionuclides took 60 min. Starting with 0.5 GBq (13.5 mCi) of ^{68}Ga, specific activities of 37–44 MBq/nmol (1–1.2 mCi/nmol) of peptide were obtained and preparations contained <3 ppm ^{68}Ge contamination. Labeling with commercially available ^{67}Ga and ^{177}Lu resulted in 20–22 and 35–40 MBq/nmol, respectively. The radiochemical purity of ^{67}Ga-BZH3, as assessed by reversed-phase HPLC, showed a
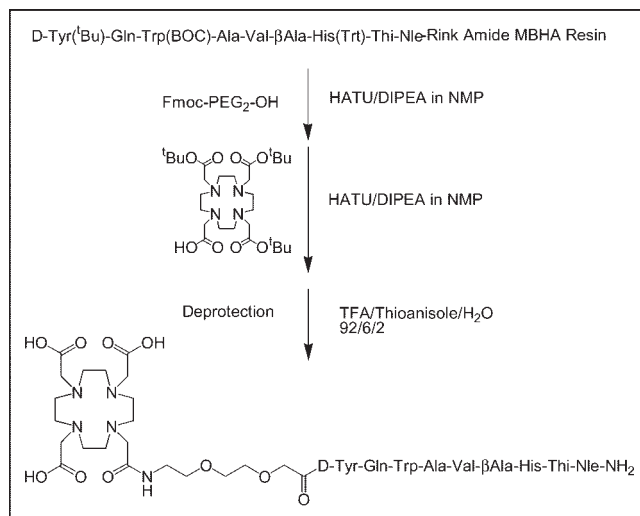

FIGURE 1. Synthesis of DOTA-PEG$_2$-[D-Tyr^6,βAla^{11},Thi^{13},Nle^{14}] BN(6–14) amide (BZH3). Thi = 3-(2-thienyl)-L-alanine; MBHA = 4-methylbenzhydrylamine; HATU = O-(7-azabenzotriazole-1-yl)-1,1,3,3-tetramethyluronium hexafluorophosphate; DIPEA = diisopropylethylamine; NMP = N-methylpyrrolidone.

single product with a slightly reduced retention time of 12.2 min versus 12.6 min for the unlabeled BZH3. Heating to 90°C during the labeling procedure caused no detectable degradation of the peptide, a finding that has also been reported by Breeman et al. (*14*). Thus, subsequent preparations were only checked by paper chromatography for the nonchelated fraction of the radionuclide that remains at the beginning. Typically, ≥98% of the activity migrated with an R$_f$ of 0.6–0.7 corresponding to the labeled peptide.

Receptor Binding

The saturation binding curve of ^{67}Ga-BZH3 to GRP-r of AR42J cells and its Scatchard transformation are shown in Figure 2. From the Scatchard plot, a high receptor affinity K$_a$ of 2.19×10^9 L/mol was calculated, which corresponds to a dissociation constant K$_d$ of 0.46 nmol/L. Determination of B$_{max}$ resulted in 9.7×10^4 receptors per cell. Nonspecific binding of the peptide was tested with the GRP-r–negative breast carcinoma cell line AR-1 and amounted to <3.5%.

Internalization

Internalization of ^{67}Ga-BZH3 by AR42J cells at 2 different concentrations was followed for 2 h (Fig. 3). The fraction of internalized activity compared with total cell-associated activity (cell surface bound + internalized) was nearly identical for both the low and the high concentration and amounted to 71%–75% after a 15- and 30-min incubation and 85%–88% after a 1- and 2-h incubation. The kinetics of internalization during the first hour of incubation also were very similar. In contrast, using the low dose and a 2-h incubation, which reduced the free peptide concentration in the medium to ≤0.02 nmol/L, the internalization rate drastically decreased.

FIGURE 2. Saturation curve (A) and Scatchard transformation (B) of binding of increasing amounts of ^{67}Ga-BZH3 to 4×10^5 AR42J cells. Cells were incubated for 1 h. Data are means of triplicate samples and are corrected for nonspecific binding ($\leq$3.5%).
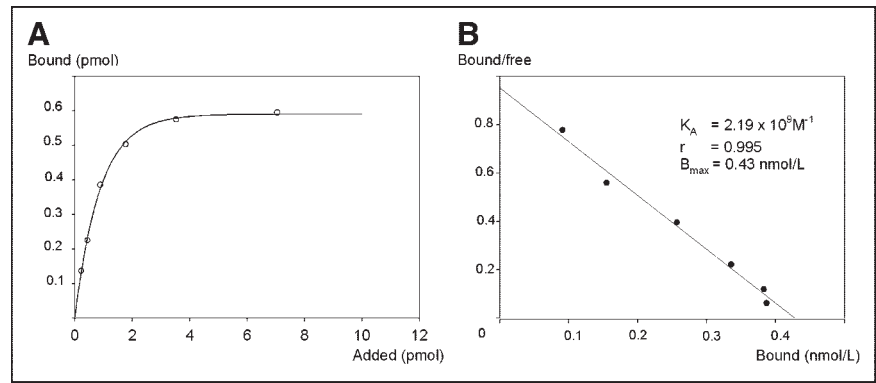
Efflux

Efflux of internalized radioactivity was evaluated after preloading of AR42J cells with either ^{67}Ga- or ^{177}Lu-labeled BZH3. Cell surface–bound peptide was removed by excess unlabeled peptide within the first minutes of incubation and amounted to ~10% of total activity, a fraction that is consistent with the results obtained in internalization experiments using an acid treatment of cells. Another ~10% was excreted during the following 2-h incubation. From a semilogarithmic plot of data, half-lives of 16.5 ± 2.4 h and 12.8 ± 1.4 h for the excretion of ^{67}Ga and ^{177}Lu, respectively, were calculated (Fig. 4).

Receptor Density

Three separate tumor inoculations (dose dependence, biokinetics, and PET) were performed with AR42J cells that differ in the number of passages from 7 to 16 relating to the commercially obtained cells. No marked difference in pep-

tide uptake was noted. The uptake amounted to 0.132, 0.145, and 0.159 pmol per 10^6 cells, respectively.

Biodistribution

Tumor and normal tissue uptake 1 h after the administration of increasing doses (5, 15, 45, and 135 pmol) of ^{67}Ga-BZH3 are presented in Table 1. A dose dependence was noted in the AR42J tumor and the normal GRP-r–expressing tissues, including small intestine, colon, and pancreas. Small intestine and colon showed a continuously decreasing uptake with increasing doses. The uptake in
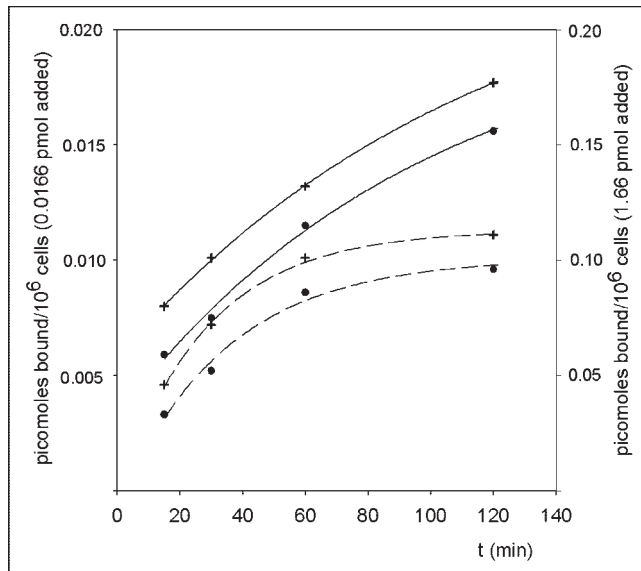

FIGURE 3. Internalization of ^{67}Ga-BZH3 by 1×10^6 AR42J cells in 300 μL medium containing either 0.0166 pmol (low dose, dashed line) or 1.66 pmol (high dose, solid line) of peptide. +, Total activity (cell surface bound + internalized); ●, internalized activity. Note different scaling of the y-axis. Data are means of triplicate samples.
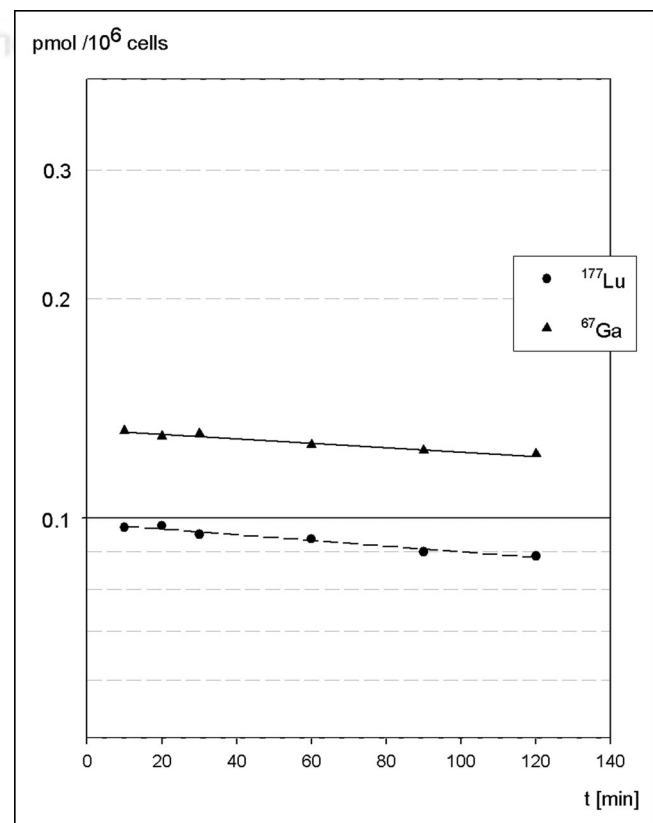

FIGURE 4. Semilogarithmic plot shows efflux (externalization) of radioactivity from AR42J cells preloaded with either ^{67}Ga-BZH3 (solid line) or ^{177}Lu-BZH3 (dashed line). Data are means of duplicate samples from 2 experiments.

TABLE 1
Tissue Distribution of Increasing Doses of ^{67}Ga-BZH3 at 1 Hour After Injection in AR42J Tumor-Bearing Nude Mice

Tissue	pmol per animal			
	5	15	45	135
Blood	0.45 ± 0.12	0.57 ± 0.17	0.51 ± 0.14	0.53 ± 0.10
Liver	0.68 ± 0.18	1.12 ± 0.39	0.87 ± 0.23	0.72 ± 0.13
Spleen	2.14 ± 0.49	1.62 ± 0.48	1.82 ± 0.89	1.29 ± 0.54
Kidneys	6.55 ± 1.92	6.32 ± 2.00	4.52 ± 0.59	3.03 ± 0.45
Pancreas	35.98 ± 2.22	40.39 ± 2.81*	46.06 ± 3.51*	39.37 ± 4.57*
Muscle	0.16 ± 0.05	0.13 ± 0.04	0.20 ± 0.07	0.20 ± 0.05
Bone[†]	0.37 ± 0.13	0.51 ± 0.22	0.29 ± 0.15	0.48 ± 0.24
Lungs	0.60 ± 0.17	0.63 ± 0.25	0.56 ± 0.15	0.64 ± 0.11
Tumor	7.98 ± 1.57	10.90 ± 1.48*	8.00 ± 1.68*	6.25 ± 0.80
Small intestine[‡]	8.70 ± 2.39	7.51 ± 1.45	5.62 ± 0.79	4.00 ± 0.43
Large intestine[‡]	3.94 ± 0.24	3.82 ± 0.49	2.96 ± 0.69	1.95 ± 0.49

*Significantly different ($P \leq 0.05$) from preceding group (Student t test).
[†]One femur was measured.
[‡]Small and large intestines were measured with content.
All data are mean percentage injected dose per gram (%ID/g) ± SD of 5 animals. Body weight of animals, 23.9 ± 1.7 g; tumor weight, 218 ± 104 mg (range, 88–388 mg); pancreas weight, 204 ± 30 mg (n = 20).

pancreas and tumor showed a bell-shaped dose dependence. The maxima obtained were 10.9 percentage injected dose per gram (%ID/g) for tumor and 46.1 %ID/g for pancreas after administration of a 15- and a 45-pmol dose, respectively. No dose dependence was found in blood, liver, spleen, muscle, lung, and bone. In kidneys, a significantly reduced activity was noted after the administration of the highest dose (135 pmol = 0.23 μg).

The tissue distribution of [67]Ga- or ^{177}Lu-labeled BZH3 as a function of time was determined using the 15-pmol dose (Table 2). The radioactivity in the GRP-r–expressing tissues after administration of the ^{67}Ga-BZH3 did not signif-

icantly decrease up to 4 h after injection. From data at 1 and 24 h after injection, the average half-lives of ^{67}Ga-BZH3 retention in pancreas and tumor of ~22 h and ~16 h could be estimated, respectively, the latter being very similar to the excretion half-life of ^{67}Ga activity in vitro after internalization of ^{67}Ga-BHZ3 into AR42J cells. Low activity was found in blood, liver, lung, muscle, and bone, even at 1 h after injection, and tumor-to-tissue ratios did not markedly increase after 2 h following injection (Table 3).

The difference in tumor uptake 1 h after injection between the 2 experiments using a 15-pmol dose, 10.9 %ID/g (dose dependence) versus 5.6 %ID/g (kinetics), is not

TABLE 2
Tissue Distribution of [67]Ga- and ^{177}Lu-BZH3 as Function of Time in AR42J Tumor-Bearing Nude Mice After Injection of 15 pmol of Peptide

Tissue	[67]Ga				[177]Lu	
	1 h	2 h	4 h	24 h	1 h	24 h
Blood	0.25 ± 0.02	0.17 ± 0.03	0.12 ± 0.01	0.015 ± 0.006	0.51 ± 0.06	0.025 ± 0.006
Liver	0.47 ± 0.12	0.40 ± 0.05	0.32 ± 0.07	0.22 ± 0.03	0.62 ± 0.06	0.35 ± 0.05
Spleen	3.32 ± 0.90	3.35 ± 1.44	2.26 ± 1.07	0.83 ± 0.24	1.67 ± 0.17	0.31 ± 0.07
Kidneys	6.78 ± 0.40	4.49 ± 0.37	4.12 ± 0.70	1.75 ± 0.40	4.96 ± 0.87	0.72 ± 0.04
Pancreas	42.16 ± 2.30	37.52 ± 6.69	36.54 ± 5.19	20.75 ± 5.24	31.78 ± 3.69	3.71 ± 0.55
Muscle	0.13 ± 0.07	0.11 ± 0.09	0.04 ± 0.02	0.021 ± 0.009	0.13 ± 0.02	0.02 ± 0.005
Bone*	0.39 ± 0.09	0.29 ± 0.03	0.26 ± 0.06	0.20 ± 0.09	0.59 ± 0.08	0.79 ± 0.13
Lungs	0.31 ± 0.04	0.19 ± 0.04	0.13 ± 0.03	0.04 ± 0.01	0.45 ± 0.06	0.05 ± 0.02
Tumor	5.65 ± 0.73	6.47 ± 1.13	5.26 ± 1.30	2.10 ± 0.38	4.52 ± 0.57	1.48 ± 0.23
Small intestine[†]	4.74 ± 0.48	3.39 ± 0.38	1.66 ± 0.18	0.85 ± 0.13	4.62 ± 0.95	0.48 ± 0.15
Large intestine[†]	4.93 ± 1.13	6.78 ± 0.93	4.90 ± 0.52	1.75 ± 0.86	3.38 ± 1.18	1.22 ± 0.14

*One femur was measured.
[†]Small and large intestines were measured with content.
All data are mean %ID/g ± SD of 5 animals. Body weight of animals, 22.4 ± 2.02 g; tumor weight, 252 ± 130 mg (range, 86–612 mg); pancreas weight, 179 ± 36 mg (n = 30).

TABLE 3
Tumor-to-Tissue Ratios of [67]Ga- and ^{177}Lu-BZH3 in Tumor-Bearing Nude Mice

Tumor/organ	[67]Ga				[177]Lu	
	1 h	2 h	4 h	24 h	1 h	24 h
Blood	22.6 ± 2.4	38.1 ± 8.5	43.8 ± 11.7	140 ± 81	8.9 ± 1.5	59 ± 23
Liver	12.0 ± 1.8	16.2 ± 1.8	16.4 ± 6.0	9.5 ± 2.3	7.3 ± 0.8	4.2 ± 1.0
Spleen	1.7 ± 0.6	1.8 ± 0.6	2.3 ± 1.0	2.5 ± 0.7	2.7 ± 0.3	4.8 ± 1.3
Kidneys	0.83 ± 0.05	1.4 ± 0.2	1.3 ± 0.4	1.2 ± 0.3	0.91 ± 0.28	2.1 ± 0.3
Pancreas	0.13 ± 0.01	0.17 ± 0.04	0.14 ± 0.05	0.10 ± 0.02	0.14 ± 0.02	0.40 ± 0.10
Muscle	74 ± 30	83 ± 26	131 ± 57	105 ± 28	34.8 ± 10.8	74 ± 39
Bone	14.5 ± 0.8	22.3 ± 3.9	20.2 ± 1.7	10.5 ± 1.5	7.7 ± 0.6	1.9 ± 0.5
Lungs	18.2 ± 3.1	34.1 ± 4.7	40.5 ± 15.0	52 ± 14	10.0 ± 1.5	30.7 ± 11.6

Ratios are calculated from animals of Table 2. Data are mean ± SD ($n = 5$).

readily understood because AR42J cells used for tumor inoculation showed no difference with regard to in vitro binding and internalization of ^{67}Ga-BZH3. A possible explanation might be that the fraction of tumor cells in relation to the total tumor mass was different, since tumors were highly hemorrhagic.

As an estimate for therapeutic applications, BZH3 was labeled with ^{177}Lu, which is a medium-energy β-emitter ($E_{β\text{-max}} = 497$ keV) with a low abundance of γ-radiation at 113 and 208 keV, and biodistribution of ^{177}Lu-BZH3 was determined at 1 and 24 h after injection of a 15-pmol dose (Table 2). Uptake in the tumor and pancreas 1 h after injection appears to be somewhat lower compared with that of ^{67}Ga-BZH3, 4.5 versus 5.6 %ID/g and 31.8 versus 42.1 %ID/g, respectively. The in vivo half-life of ^{177}Lu-BZH3 in the tumor, estimated from the 1- and 24-h biodistribution data, was ~14 h and, thus, corresponds to the in vitro data of efflux. In contrast, the decline of ^{177}Lu activity in the pancreas was significantly accelerated compared with that of the ^{67}Ga-labeled BZH3 ($t_{1/2}$, ~7.5 vs. ~22 h).

Coadministration of excess unlabeled BZH3 in the blocking experiments reduced uptake of ^{177}Lu-BZH3 in the pancreas of rats from 2.69 ± 0.60 %ID/g to 0.06 ± 0.01 %ID/g and in the AR42J tumor from 1.11 ± 0.31 %ID/g to 0.09 ± 0.01 %ID/g, indicating a specific and GRP-r–mediated uptake of the labeled peptide.

PET

PET images of tumor-bearing mice obtained 1 h after injection of 15 pmol ^{68}Ga-BZH3 are presented in Figure 5. Transaxial slices cutting the tumor and mediastinal region demonstrate a clear delineation of the tumor tissue and a low activity background in lungs, liver, and circulation. Coronal slices show the highest activity in pancreas and a nonuniform activity distribution in the duodenum, which complicates visualization of the kidneys. γ-Counting indicated an activity accumulation of 5.3 and 7.0 %ID/g in the resected tumors of the left and the right animal, respectively. Tumor weights were 200 mg (left animal) and 128 mg (right animal).

DISCUSSION

During the past decade, the successful application of radiolabeled somatostatin analogs in nuclear medicine for diagnostics and therapy of neuroendocrine tumors has stimulated the research in receptor targeting of additional tumor types (26). In a recent study, Van de Wiele et al. demonstrated the feasibility of scintigraphic imaging of GRP-r–positive prostate and breast carcinoma in patients with the [99m]Tc- labeled BN analog RP 527, indicating the potential of BN analogs for use in humans (13,27). In the present study, we investigated a novel BN analog, BZH3, for its in vitro and in vivo behavior under the aspects of improving targeting of GRP-r–positive tumors and introducing the short-lived positron emitter ^{68}Ga for peptide labeling and, thus, to enable PET, which increases the spatial resolution and sensitivity of tumor detection compared with conventional γ-camera imaging (28–30). Additionally, scatter-corrected PET provides the ability to quantify biodistribution and, thus, may be favorably used for GRP-r density determination, which is a prerequisite for the appropriate selection of patients entering radiotherapy, and to control effectiveness of radiotherapy or surgical interventions.

The affinity of ^{67}Ga-BZH3 to GRP-r of live AR42J cells showed a K_d of 0.46 nmol/L, which is a factor of 3 lower
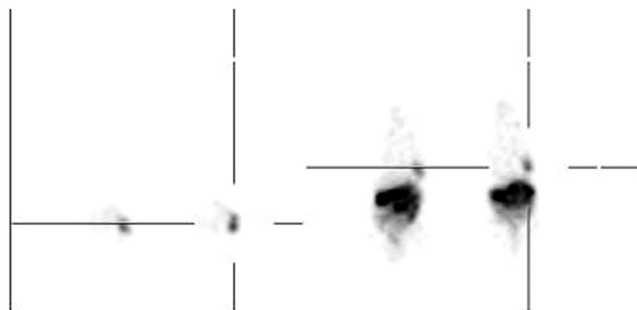

FIGURE 5. Iteratively reconstructed transaxial (left) and coronal (right) PET images of 2 AR42J tumor-bearing nude mice 1 h after injection of 15 pmol (0.49 MBq) ^{68}Ga-BZH3. Tumors are located in thoracic wall. Tumor uptake and weight: left animal, 5.3 %ID/g, 200 mg; right animal, 7.0 %ID/g, 128 mg.

than that of ^{125}I-Tyr^4-BN (K$_d$ = 1.6 nmol/L), which is commonly used as a standard for determination of GRP-r–specific binding. The affinity of ^{67}Ga-BZH3 is thus comparable with that of ^{99m}Tc-demobesin 1 (K$_d$ = 0.67 nmol/L) (18) and ^{111}In-labeled DOTA-Aoc-BN(7–14) (50% inhibitory concentration = 0.6 nmol/L vs. ^{125}I-Tyr^4-BN) (15), which are the BN analogs with the highest GRP-r affinity reported so far. Though determination of K$_d$ is independent of using live cells or cell membranes (31), the B$_{max}$ of 9.7 × 10^4 receptors per cell, obtained with live AR42J cells, overestimates the number of receptors actually present on the cell surface. This can be attributed to the recycling of part of the receptors to the cell surface after internalization of the GRP-r/BN complex (27,32), which increases the B$_{max}$ of live cells with incubation time.

Internalization of ^{67}Ga-BZH3 into AR42J cells suggests an agonistic nature of the peptide. The rapid and high degree of internalization—70% of total cell-associated activity was endocytosed within 15 min using both the low and the high peptide concentration—fits well with the internalization rate of the agonist ^{125}I-Tyr^4-BN/GRP-r complex (t$_{1/2}$ ~ 6 min) and its independence from the peptide-to-receptor ratio (31).

Efflux of ^{67}Ga and ^{177}Lu activity from AR42J cells after internalization of labeled BZH3 showed half-lives of 13–16 h in vivo and in vitro, which are much longer than that of ^{125}I-Tyr^4-BN (t$_{1/2}$ ~ 3 h) (33). Since lysosomal degradation of BN analogs is very rapid—after a 15 min-incubation, 80% of internalized ^{125}I-Tyr^4-BN has already been metabolized (34)—the prolonged intracellular retention in tumor cells appears to be a specific feature of the M^{3+} DOTA chelate and presumably of the linker used for coupling rather than of the peptide degradation products. This is supported by similar efflux data of ^{177}Lu from PC-3 tumor cells using a different, but DOTA-conjugated, BN analog (35).

Biodistribution studies with escalating doses of ^{67}Ga-BZH3 in tumor-bearing mice indicated a dose-dependent uptake in GRP-r–positive tissues. Intestines showed a continuously decreasing %ID/g uptake with increasing amounts of peptide, which indicates an increasing saturation of the receptors and an uptake maximum equal to or less than the lowest dose of 5 pmol per animal. In contrast, tumor and pancreas uptake peaked at the 15- and 45-pmol dose, respectively. Breeman et al. (36) also described such a bell-shaped, dose-dependent uptake in the pancreas of rats. These authors suggest that the initial stimulation of the %ID/g uptake with increasing amounts of peptide might be related to a clustering of the receptor/BN complexes in the cell membrane, which might be required for internalization of the complexes. Since we found no dose dependence of internalization in vitro with doses much lower than that used in biodistribution experiments, in vivo a preferential trapping of the peptide at low doses in the intestines appears to be more likely. Assuming receptor densities of pancreas > tumor > intestine—but taking into account the high abso-lute amount of intestinal GRP-r and a much higher blood flow in the intestines compared with the tumor tissue (37)—an optimum tumor uptake may be achieved only after a sufficient saturation of the intestinal GRP-r. In GRP-r–negative tissues, only kidneys showed a significantly reduced activity uptake after administration of the highest dose. This is in contrast to published results reporting no change in the kidney uptake of BN analogs in mice and rats up to a 100-μg dose (36,37). Thus, a slightly prolonged retention time of the small doses of ^{67}Ga-BHZ3 in the kidneys seems to be more likely than a saturation of renal excretion by the high dose.

The clearance of ^{67}Ga-BZH3 from the circulation and normal GRP-r–negative tissues was fast and resulted in low background activity with maximum tumor-to-tissue ratios at 2 h after injection, which meets the requirements of PET with the short-lived positron emitter ^{68}Ga. The low liver uptake of 0.5 %ID/g versus 3–8 %ID/g observed for ^{99m}Tc-labeled BN analogs (17,18,33,38) should facilitate tumor localization in the abdominal region compared with ^{99m}Tc imaging.

Similar to somatostatin analogs, BN analogs labeled with a therapeutic radionuclide might have a potential for radiotherapy. Using the diagnostic radiolabel for calculation of the absorbed therapeutic radiation dose, a comparison of the biokinetics of the therapeutic and the diagnostic radiolabel is necessary, since a change in the M^{3+} radiometal used for DOTA labeling can alter the biodistribution of a DOTA-conjugated peptide (39). For the couple of $^{67/68}$Ga and ^{177}Lu (the latter has been used successfully in therapy of neuroendocrine tumors (40)), we found a slightly reduced (~20%) uptake of ^{177}Lu-BZH3 in the tumor and a ~20% shortened half-life of tumor retention, whereas biodistribution and biokinetics in normal tissues were quite similar to that of ^{67}Ga-BZH3. An exception, which might be beneficial for therapy, is the observed 3-fold accelerated clearance of pancreatic ^{177}Lu activity. Presently, no reasonable explanation for the different kinetics of the ^{67}Ga- and ^{177}Lu-labeled peptide could be found. However, the data are in agreement with those reported by Smith et al. (35) for the washout of ^{177}Lu activity from the pancreas of mice after administration of the ^{177}Lu DOTA-8-Aoc-BN(7–14) analog. Nevertheless, the high initial, receptor-mediated ^{177}Lu uptake in the pancreas has to be considered for limiting-dose calculations.

PET clearly indicated the potential of ^{68}Ga-BZH3 for a sensitive localization of GRP-r–positive tumors in the mediastinal area. Compared with a ^{64}Cu-labeled DOTA-BN analog (t$_{1/2}$, 12.7 h; β$^+$, 19%), recently proposed for PET (37), ^{68}Ga-BZH3 appears to be much more favorable with regard to in vivo stability and biodistribution, in vitro data, and simplicity of radionuclide production. Detection of metastatic prostate carcinoma, especially of an invasion of pelvic lymph nodes, remains less predictable because of the enhanced intestinal and bladder background activity. On the other hand, the high GRP-r density found in most of the

prostatic neoplasms and metastases (*8*) might partially compensate these limitations.

CONCLUSION

The M^{3+} radiolabeled BN analog BZH3 evaluated in this study has shown many of the prerequisites for a successful targeting of GRP-r–positive tumors, such as a high affinity in the subnanomolar range and a rapid internalization with a prolonged intracellular retention of the M^{3+} radionuclide in vitro. In vivo, high tumor-to-tissue ratios 1 h after injection and a rapid clearance of unbound peptide from GRP-r–negative, normal tissues was observed. PET has demonstrated the diagnostic potential in the tumor-bearing mouse model with ^{68}Ga-BZH3. Additionally, the ability of PET to quantify biodistribution data should enable more accurate dose calculations for radiotherapy with M^{3+} therapeutic radionuclides—for example, ^{90}Y or ^{177}Lu. The physiologic features together with PET and the simplicity of ^{68}Ga production from a generator recommend ^{68}Ga-BZH3 as a promising, versatile tool for an improved localization of GRP-r–positive tumors also in patients.

Because our generator is not commercially available, we refer the reader to a TiO_2-based ^{68}Ge/^{68}Ga generator, which is commercially available from the Cyclotron Co. Ltd. Obninsk. Meyer et al. (*41*) have published a comparison, showing a similar suitability and efficiency of both generators.

REFERENCES

1. Martinez V, Tache Y. Bombesin and the brain-gut axis. *Peptides.* 2000;21:1617–1625.
2. Delle Fave G, Annibale B, De Magistris L, et al. Bombesin effects on human GI functions. *Peptides.* 1985;6:113–116.
3. Cuttita F, Carney DN, Mulshine J, et al. Bombesin-like peptides can function as autocrine growth factors in human small cell lung cancer. *Nature.* 1985;316:823–826.
4. Bologna MC, Festuccia C, Muzi P, Biordi L, Ciomei M. Bombesin stimulates growth of human prostatic cancer cells in vitro. *Cancer.* 1989;63:1714–1720.
5. Yano T, Pinski J, Groot K, Schally AV. Stimulation by bombesin and inhibition by bombesin/gastrin-releasing peptide antagonist RC-3095 of growth of human breast cancer cell lines. *Cancer Res.* 1992;52:4545–4547.
6. Gugger M, Reubi JC. Gastrin-releasing peptide receptors in non neoplastic and neoplastic human breast. *Am J Pathol.* 1999;155:2067–2076.
7. Reubi JC, Gugger M, Waser B. Co-expressed peptide receptors in breast cancer as a molecular basis for in vivo multireceptor tumor targeting. *Eur J Nucl Med.* 2002;29:855–862.
8. Markwalder R, Reubi JC. Gastrin releasing peptide receptors in human prostate: relation to neoplastic transformation. *Cancer Res.* 1999;59:1152–1159.
9. Reubi JC, Wenger S, Schmuckli-Maurer J, Schaer JC, Gugger M. Bombesin receptor subtypes in human cancers: detection with the universal radioligand ^{125}I-[D-Tyr^6,β Ala^{11},Phe^{13},Nle^{14}]bombesin(6–14). *Clin Cancer Res.* 2002;8:1139–1146.
10. Reubi JC, Waser B. Concomittant expression of several peptide receptors in neuroendocrine tumors: molecular basis for in vivo multireceptor tumor targeting. *Eur J Nucl Med.* 2003;30:781–793.
11. Moody TW, Carney DN, Cuttita F, Quattrocchi K, Minna JD. High affinity receptors for bombesin/GRP-like peptides on human small cell lung cancer. *Life Sci.* 1985;37:105–113.
12. Reubi JC, Körner M, Waser B, Mazzucchelli L, Guillou L. High expression of peptide receptors as novel target in gastrointestinal stromal tumours. *Eur J Nucl Med.* 2004;31:803–810.
13. Van de Wiele C, Dumont F, Van den Broecke R, et al. Technetium-99m RP527, a GRP analogue for visualisation of GRP receptor-expressing malignancies: a feasibility study. *Eur J Nucl Med.* 2000;27:1694–1699.
14. Breeman WAP, de Jong M, Erion JL, et al. Preclinical comparison of ^{111}In-labeled DTPA- or DOTA-bombesin analogs for receptor targeted scintigraphy and radionuclide therapy. *J Nucl Med.* 2002;43:1650–1656.
15. Hoffman TJ, Gali H, Smith CJ, et al. Novel series of In-111 labeled bombesin analogs as potential radiopharmaceuticals for specific targeting of gastrin-releasing peptide receptors expressed on human prostate cancer cells. *J Nucl Med.* 2003;44:823–831.
16. Van de Wiele C, Dumont F, Dierckx RA, et al. Biodistribution and dosimetry of ^{99m}Tc-RP 527, a gastrin-releasing peptide (GRP) agonist for the visualization of GRP receptor-expressing malignancies. *J Nucl Med.* 2001;42:1722–1727.
17. Smith CJ, Sieckman GL, Owen NK, et al. Radiochemical investigations of gastrin-releasing peptide receptor-specific [^{99m}Tc (X) (CO)$_3$-Dipr-Ser-Ser-Ser-Gln-Trp-Ala-Val-Gly-His-Leu-Met(NH$_2$)] in PC-3, tumor-bearing, rodent models: syntheses, radiolabeling, and in vitro/in vivo studies where Dpr = 2,3-diaminopropionic acid and X = H_2O or P(CH_2OH)$_3$. *Cancer Res.* 2003;63:4082–4088.
18. Nock B, Nikolopoulou A, Chiotellis E, et al. ^{99m}Tc-Demobesin 1, a novel potent bombesin analogue for GRP receptor-targeted tumor imaging. *Eur J Nucl Med.* 2003;30:247–258.
19. Scopinaro F, DeVincentis G, Varvarigou AD, et al. ^{99m}Tc-Bombesin detects prostate cancer and invasion of pelvic lymph nodes. *Eur J Nucl Med.* 2003;30:1378–1382.
20. Smith CJ, Sieckman GL, Owen NK, et al. Radiochemical investigations of [^{188}Re(H_2O)(CO)$_3$-diaminopropionic acid-SSS-bombesin(7–14) NH$_2$]: syntheses, radiolabeling and in vitro/in vivo GRP receptor targeting studies. *Anticancer Res.* 2003;23:63–70.
21. Eisenwiener KP, Prata MI, Buschmann I, et al. NODAGATOC, a new chelator-coupled somatostatin analogue labeled with $^{67/68}$Ga and ^{111}In for SPECT, PET, and targeted therapeutic applications of somatotastin receptor (hsst2) expressing tumors. *Bioconjug Chem.* 2002;13:530–541.
22. Schuhmacher J, Maier-Borst W. A new Ge-68/Ga-68 radioisotope generator system for production of Ga-68 in dilute HCl. *Int J Appl Radiat Isot.* 1981;32:31–36.
23. Presky DH, Schonbrunn A. Somatostatin pretreatment increases the number of somatostatin receptors in GH$_4$C$_1$ pituitary cells and does not reduce cellular responsiveness to somatostatin. *J Biol Chem.* 1988;263:714–721.
24. Zhang H, Chen J, Waldherr C, et al. Synthesis and evaluation of bombesin derivatives on the basis of pan-bombesin peptides labeled with In-111, Lu-177 and Y-90 for targeting bombesin receptor-expressing tumors. *Cancer Res.* 2004;64:6707–6715.
25. Doll J, Henze M, Bublitz O, et al. High resolution reconstruction of PET images using the iterative OSEM algorithm. *Nuklearmedizin.* 2004;43:72–79.
26. Hoffman TJ, Quinn TP, Volkert WA. Radiometallated receptor-avid peptide conjugates for specific in vivo targeting of cancer cells. *Nucl Med Biol.* 2001;28:527–539.
27. Van de Wiele C, Dumont F, Van Belle S, Slegers G, Peers SH, Dierckx RA. Is there a role for agonist gastrin-releasing peptide receptor radioligands in tumor imaging? *Nucl Med Commun.* 2000;22:5–15.
28. Henze M, Schuhmacher J, Hipp P, et al. PET imaging of somatostatin receptors using ^{68}Ga DOTA-DPhe^{1}Tyr^3 Octreotide: first results in patients with meningiomas. *J Nucl Med.* 2001;42:1053–1056.
29. Hofmann M, Mäcke HR, Börner AR, et al. Biokinetics and imaging with the somatostatin receptor PET radioligand ^{68}Ga-DOTA TOC: preliminary data. *Eur J Nucl Med.* 2001;28:1751–1757.
30. Kowalski J, Henze M, Schuhmacher J, Mäcke HR, Hofmann M, Haberkorn U. Evaluation of positron emission tomography imaging using ^{68}Ga DOTA-DPhe^1-Tyr^3-Octreotide in comparison to ^{111}In DTPA OC SPECT: first results in patients with neuroendocrine tumors. *Mol Imaging Biol.* 2003;5:42–48.
31. Tsuda T, Kusui T, Hou W, et al. Effect of gastrin releasing peptide receptor number on receptor affinity, coupling, degradation and modulation. *Mol Pharmacol.* 1997;51:721–732.
32. Tseng MJ, Detjen K, Struk V, Logsdon CD. Carboxyl-terminal domains deter-

mine internalization and recycling characteristics of bombesin receptor chimeras. *J Biol Chem.* 1995;270:18858–18864.

33. Smith CJ, Gali H, Sieckman GL, Higgenbotham C, Volkert WA, Hoffman TJ. Radiochemical investigations of ^{99m}Tc-N$_3$-S-X-BBN[7–14]NH$_2$: an in vitro/in vivo structure-activity relationship study where X = 0-, 3-, 5-, 8-, and 11-carbon tethering moieties. *Bioconjug Chem.* 2003;14:93–102.

34. Zhu WY, Göke B, Williams JA. Binding, internalization and processing of bombesin by rat pancreatic acini. *Am J Physiol.* 1991;261:G57–G64.

35. Smith CJ, Gali H, Sieckman GL, et al. Radiochemical investigations of ^{177}Lu-DOTA-8-Aoc-BBN[7–14]NH$_2$: an in vitro/in vivo assessment of the targeting ability of this new radiopharmaceutical for PC-3 human prostate cancer cells. *Nucl Med Biol.* 2003;30:101–109.

36. Breeman WAP, DeJong M, Bernard BF, et al. Pre-clinical evaluation of [^{111}In-DTPA-Pro[1],Tyr[4]]bombesin, a new radioligand for bombesin-receptor scintigraphy. *Int J Cancer.* 1999;83:657–663.

37. Rogers BE, Bigott HM, McCarthy DW, et al. Micro PET imaging of a gastrin-releasing peptide receptor-positive tumor in a mouse model of human prostate cancer using a ^{64}Cu-labeled bombesin analog. *Bioconjug Chem.* 2003;14:756–763.

38. LaBella R, Garcia-Garayoa E, Langer M, Bläuenstein P, Beck-Sickinger AG, Schubiger PA. In vitro and in vivo evaluation of a ^{99m}Tc(I)-labeled bombesin analogue for imaging of gastrin releasing peptide receptor-positive tumors. *Nucl Med Biol.* 2002;29:553–560.

39. Heppeler A, Froidevaux S, Mäcke HR, et al. Radiometal-labeled macrocyclic chelator derivatised somatostatin analogue with superb tumor targeting properties and potential for receptor mediated internal radiotherapy. *Chem Eur J.* 1999;5:1974–1981.

40. Kwekkeboom DJ, Bakker WH, Kam BL, et al. Treatment of patients with gastro-entero-pancreatic (GEP) tumours with the novel radiolabelled somatostatin analogue [^{177}Lu-DOTA(0),Tyr[3]]octreotate. *Eur J Nucl Med.* 2003;30:417–422.

41. Meyer GJ, Maecke H, Schuhmacher J, Knapp WH, Hofman M. ^{68}Ga-Labeled DOTA-derivatised peptide ligands. *Eur J Nucl Med.* 2004;31:1097–1104.